

Supporting Information for

**Flexible and Stable PEO-Based Polymer Composite Solid Electrolyte  
Membranes Incorporating NASICON-Type  $\text{Li}_{1.3}\text{Al}_{0.3}\text{Ti}_{1.7}(\text{PO}_4)_3$  for High -  
Performance All-Solid-State Lithium Batteries**

**Sumit Khatua,<sup>1,2</sup> Sasikumar K,<sup>1,2</sup> K. Ramakrushna Achary,<sup>3</sup> Gajjala Sindhu,<sup>1</sup> Tausif  
Alam,<sup>1</sup> L. N. Patro<sup>1,2\*</sup>**

*<sup>1</sup>Solid State Ionics Lab, Department of Physics, SRM University AP, Amaravati, 522240,  
Andhra Pradesh, India*

*<sup>2</sup>SRM-Amara Raja Center for Energy Storage Devices, SRM University AP, Amaravati,  
522240, Andhra Pradesh, India*

*<sup>3</sup>Department of Chemistry, SRM University AP, Amaravati, 522240, Andhra Pradesh, India*

---

\*Corresponding author: [laxminarayana.p@srmmap.edu.in](mailto:laxminarayana.p@srmmap.edu.in); patrolng@gmail.com (L. N.  
Patro)

Tel: 0863-2343000

Fax: 0863-2343111

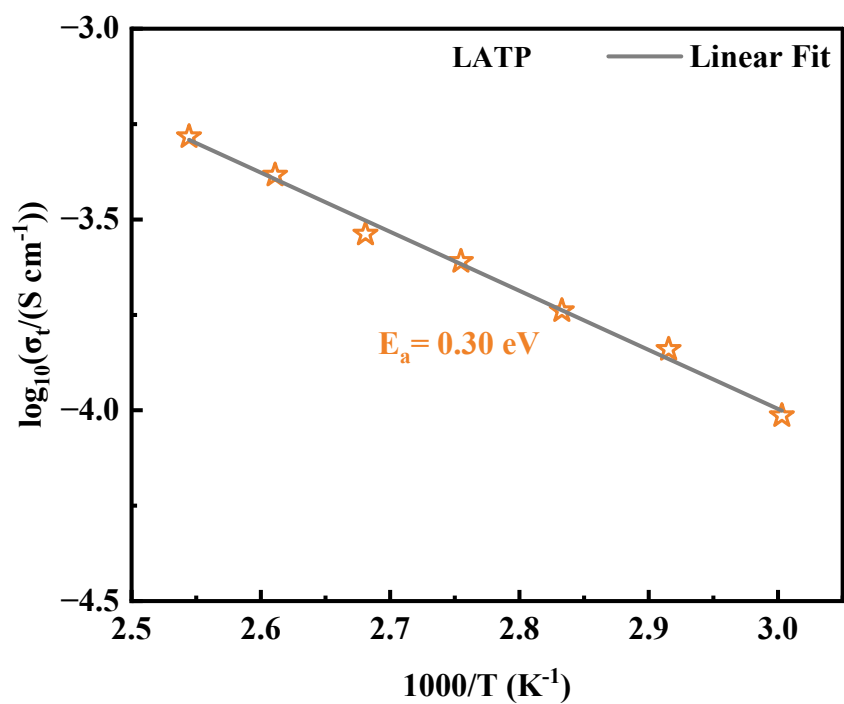
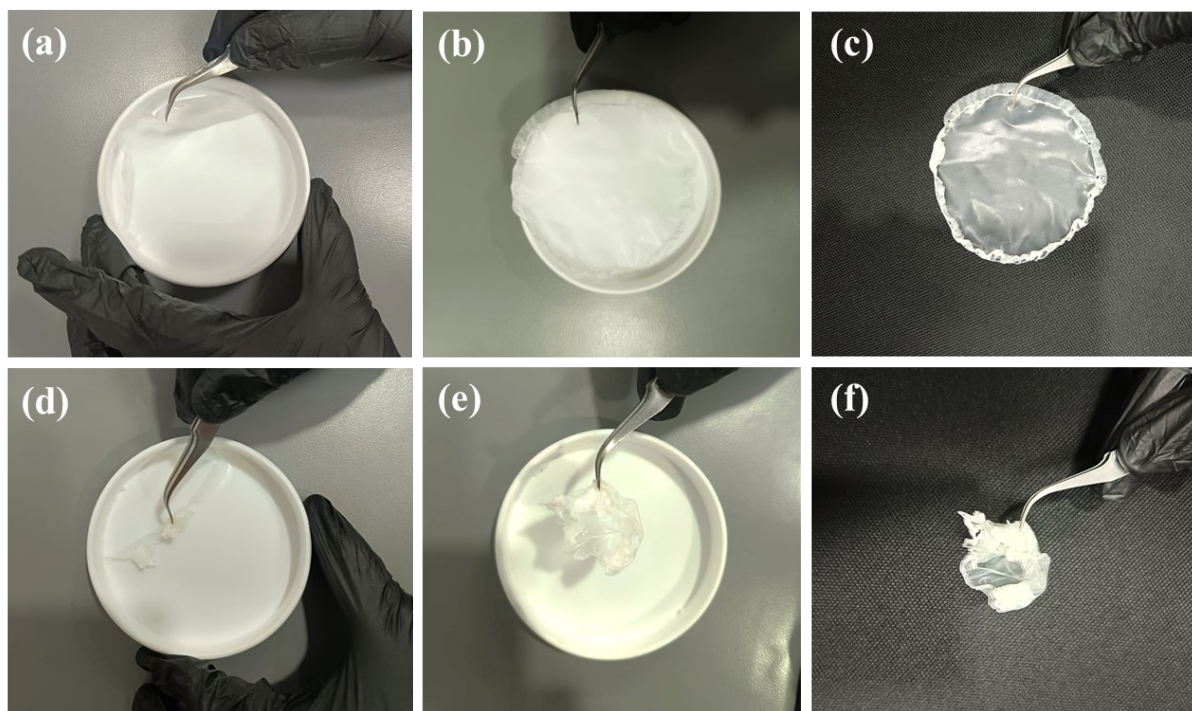
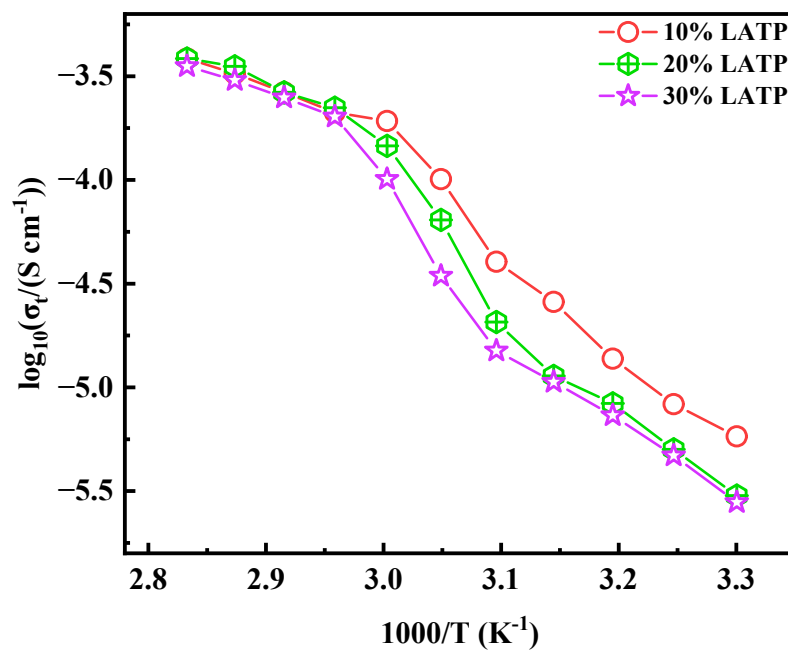


Fig. S1. Temperature dependent conductivity plot of LATP pellet.



**Fig. S2 (a-c).** Photographs of the 20% LiTFSI and **(d-f).** 25% LiTFSI polymer membranes at RT during their development.



**Fig S3.** Temperature-dependent ionic conductivity (30-80°C) of PCSE membranes with varying LATP ceramic filler concentrations.

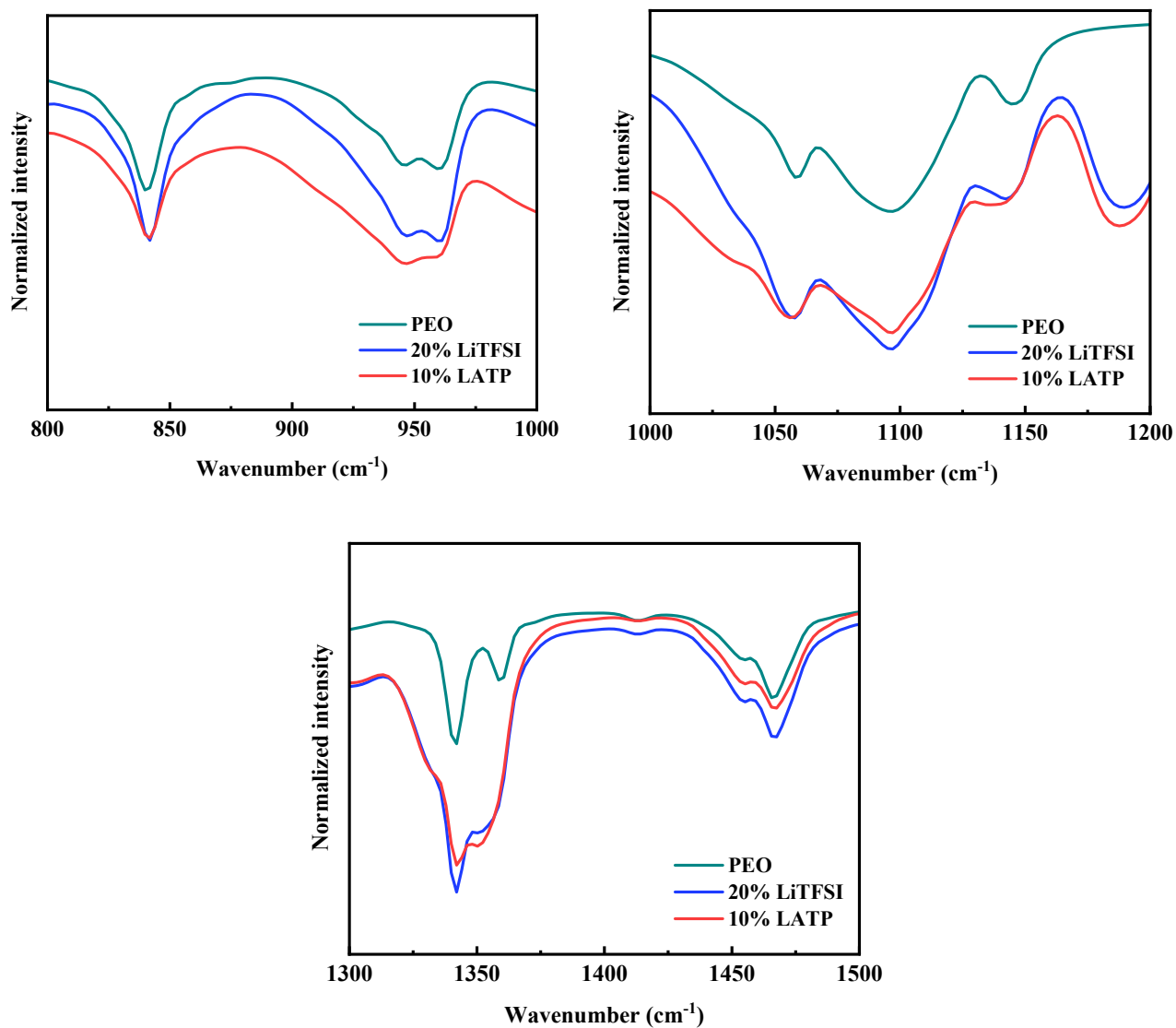


**Fig. S4.** Magnified regions of the FTIR spectra at specific wavenumber ranges.

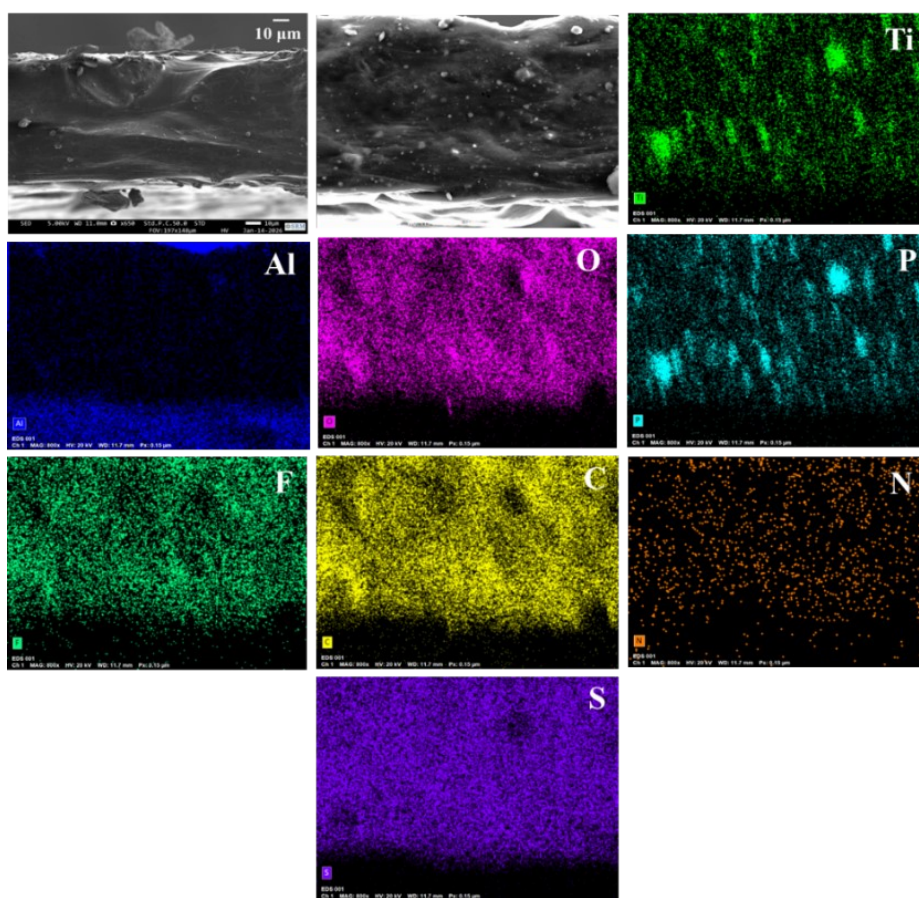


**Fig S5.** Cross-sectional SEM image with corresponding elemental mapping of the 10% LATP PCSE membrane.

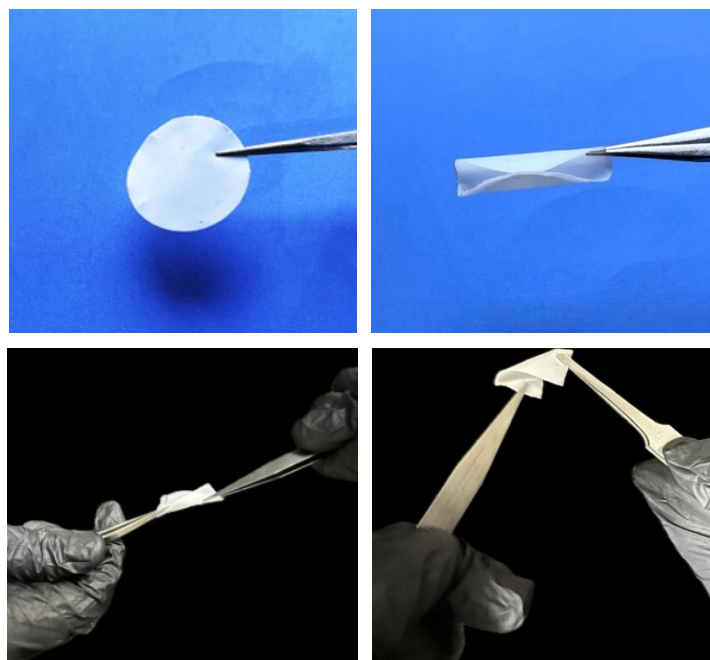


**Fig S6.** Digital photographs showing the flexibility of the 10% LATP PCSE membrane under bending and twisting tests.

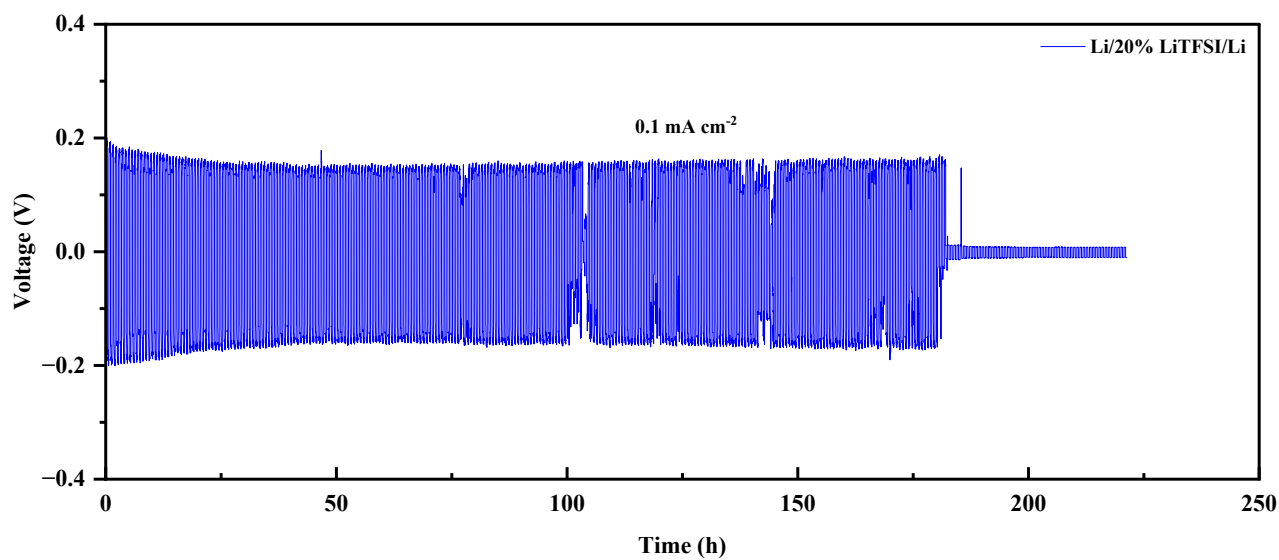


**Fig. S7.** Cycling stability of the Li/20% LiTFSI/ Li symmetric cell during lithium stripping-plating at a constant current density of 0.1 mA cm<sup>-2</sup>.

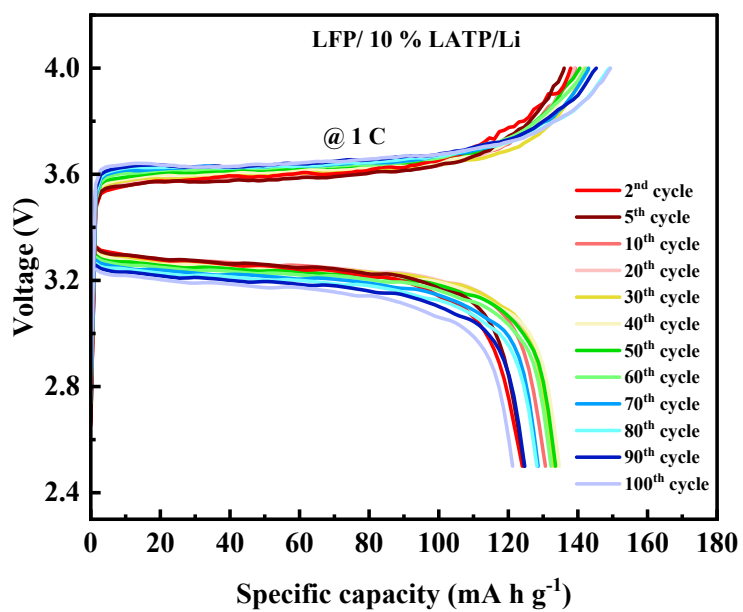


**Fig. S8.** Galvanostatic charge-discharge profiles showing the cycling performance of LFP/10% LATP/Li cell at 1 C.

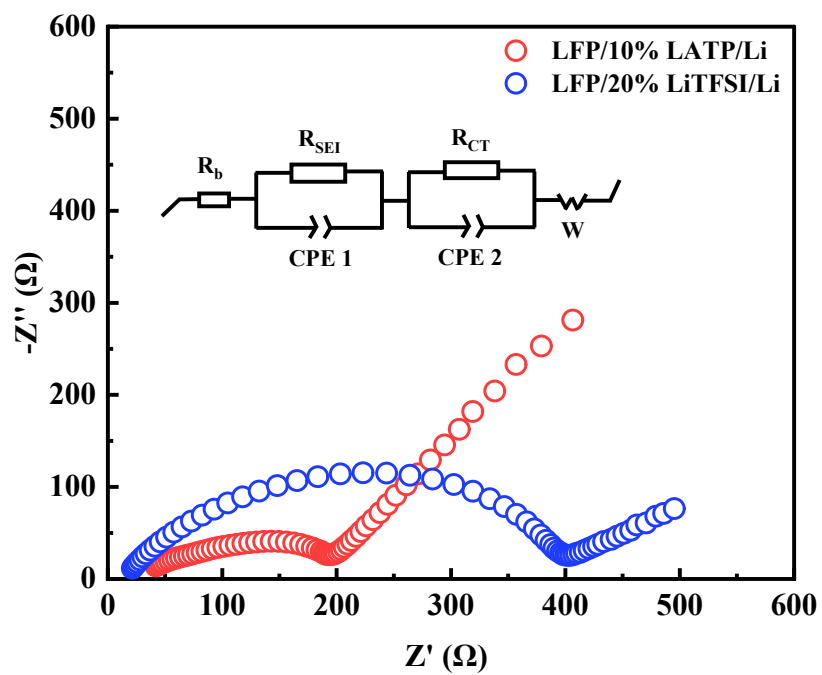


**Fig. S9.** Nyquist plots of the LFP/PCSE/Li cell before cycling at 60°C.

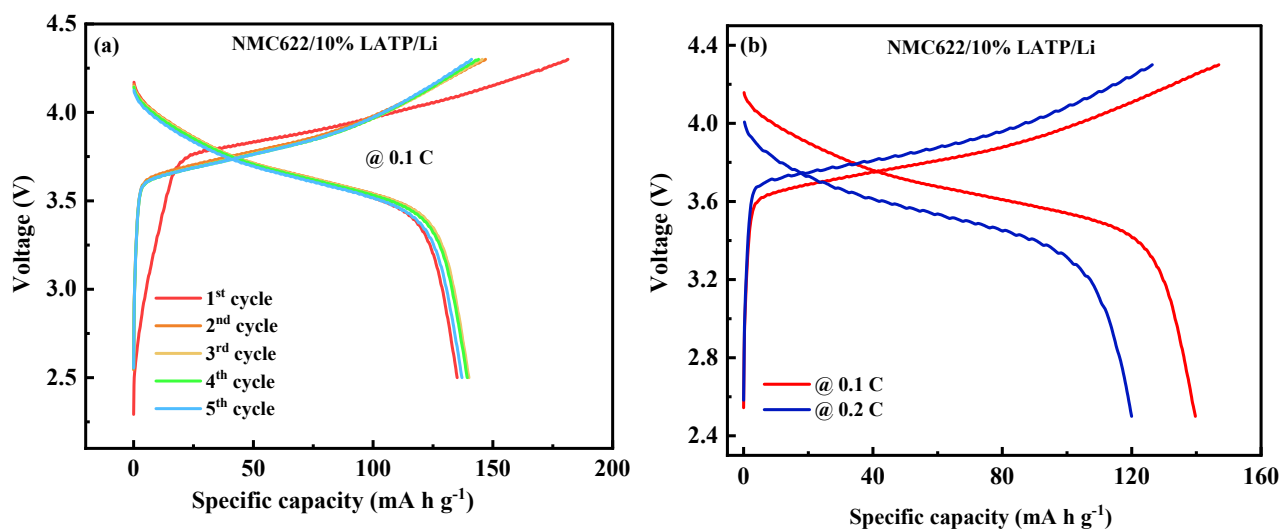


**Fig. S10(a)** Charge-discharge profiles of NMC622/10% LATP/Li cell at 0.1 C. **(b)** Charge-discharge curves of NMC622/10% LATP/Li cell at two different current rates.

**Table S1:** Conductivity values of different PEO-based polymer membranes.

<b>Sample name</b>	<b>Conductivity (RT)</b>	<b>Conductivity (60°C)</b>
	<b>(S cm<sup>-1</sup>)</b>	<b>(S cm<sup>-1</sup>)</b>
15% LiTFSI	$0.13 \times 10^{-5}$	$0.30 \times 10^{-4}$
20% LiTFSI	$0.28 \times 10^{-5}$	$0.22 \times 10^{-3}$
10% LATP	$0.34 \times 10^{-5}$	$0.19 \times 10^{-3}$
20% LATP	$0.26 \times 10^{-5}$	$0.81 \times 10^{-4}$
30% LATP	$0.22 \times 10^{-5}$	$0.49 \times 10^{-4}$

**Table S2.** Comparison of the ionic conductivity and electrochemical performance of 20% LiTFSI and 10% LATP polymer membranes with previously reported values for polymer and composite polymer electrolytes.

Polymer Electrolyte	Ionic conductivity (S cm <sup>-1</sup> )	Discharge capacity (mA h g <sup>-1</sup> ) LiFePO <sub>4</sub> //Li	Current rate	Reference
PEO-LiTFSI	2.95 × 10 <sup>-4</sup> at 55°C	151.6 at 55°C	0.2 C	<b>1</b>
PEO-LiTFSI	2.86 × 10 <sup>-4</sup> at 60°C	152.02 at 60°C	0.2 C	<b>2</b>
PVDF–HFP- LiTFSI	7.1 × 10 <sup>-5</sup> at RT	112 at RT	0.2 C	<b>3</b>
PVDF–HFP-LiTFSI	2.5 × 10 <sup>-4</sup> at 25°C	127.4 at 25°C	0.1 C	<b>4</b>
PEO-LiTFSI (20 % LiTFSI)	2.2 × 10 <sup>-4</sup> at 60°C	143.4 at 60°C	0.1 C	This work
PEO-LiClO <sub>4</sub> -LATP	1.6 × 10 <sup>-3</sup> at 80°C	130.2 at 80°C	0.2 C	<b>5</b>
PEO-LiTFSI-LATP- FEC	1.99 × 10 <sup>-4</sup> at 30°C	147 at RT	0.1 C	<b>6</b>
PEO-LiTFSI-LAGP	1.6 × 10 <sup>-5</sup> at 20°C	166 at 80°C	0.1 C	<b>7</b>
PEO-LiTFSI- LLZTO	2.12 × 10 <sup>-4</sup> at 60°C	153.8 at 60°C	0.3 C	<b>8</b>

PVDF-LiTFSI-	$2.44 \times 10^{-4}$	155	0.2 C	<b>9</b>
LATP	at 25°C	at 30°C		
PEO-LiTFSI-LATP (10% LATP)	$1.9 \times 10^{-4}$ at 60°C	151.6 at 60°C	0.1 C	This work

## References

1. E. Zhao, Y. Guo, Y. Xin, G. Xu, X. Guo, Enhanced electrochemical properties and interfacial stability of poly(ethylene oxide) solid electrolyte incorporating nanostructured  $\text{Li}_{1.3}\text{Al}_{0.3}\text{Ti}_{1.7}(\text{PO}_4)_3$  fillers for all solid state lithium ion batteries. *Int. J. Energy Res.*, 2020, **45**, 6876-6887.  
<https://doi.org/10.1002/er.6278>
2. Y. Guo, E. Zhao, W. Su, Z. Liu, J. Li, One-dimensional LATP nanofiber reinforced PEO solid composite electrolyte for all-solid-state lithium-ion batteries with excellent cycling performance. *Chem. Eng. J.*, 2025, **511**, 162127.  
<https://doi.org/10.1016/j.cej.2025.162127>
3. Y. Li, H. Wang, Composite solid electrolytes with NASICON-type LATP and PVdF-HFP for solid-state lithium batteries. *Ind. Eng. Chem. Res.*, 2021, **60**, 1494-1500.  
<https://dx.doi.org/10.1021/acs.iecr.0c05075>
4. C. Zhao, W. Wei, Z. Li, Z. Liu, Optimised sol-gel synthesis of Al-doped LLZO/PVDF-HFP/LiTFSI composite electrolytes with enhanced electrochemical performance. *Ceram. Int.*, 2025, **51**, 57807-57818.  
<https://doi.org/10.1016/j.ceramint.2025.09.481>
5. X. Ban, W. Zhang, N. Chen, C. Sun, A high-performance and durable poly(ethylene oxide) based composite solid electrolyte for all solid-state lithium battery. *J. Phys. Chem. C*, 2018, **122**, 9852-9858.

<https://doi.org/10.1021/acs.jpcc.8b02556>

6. S. Li, G. Sun, M. He, H. Li, Organic-inorganic composite electrolytes optimized with fluoroethylene carbonate additive for quasi-solid-state lithium-metal batteries. *ACS Appl. Mater. Interfaces*, 2022, **14**, 20962-20971.

<https://doi.org/10.1021/acsami.2c02038>

7. G. Piana, F. Bella, F. Geobaldo, G. Meligrana, C. Gerbaldi, PEO/LAGP hybrid solid polymer electrolytes for ambient temperature lithium batteries by solvent-free, “one pot” preparation. *J. Energy storage*, 2019, **26**, 100947.

<https://doi.org/10.1016/j.est.2019.100947>

8. L. Zhang, J. Feng, G. Zhu, J. Yan, S. Bartlett, Z. Wang, Z. Hao, Z. Gao, Effect of  $\text{Li}_{6.4}\text{La}_3\text{Zr}_{1.4}\text{Ta}_{0.6}\text{O}_{12}$  fillers on the interfacial properties between composite PEO-LiTFSI electrolytes with Li metal during cycling. *ACS Appl. Mater. Interfaces*, 2024, **16**, 13786-13794.

<https://doi.org/10.1021/acsami.3c19519>

9. L. Liu, D. Zhang, J. Zhao, J. Shen, F. Li, Y. Yang, Z. Liu, W. He, W. Zhao, J. Liu, Synergistic effect of lithium salts with fillers and solvents in composite electrolytes for superior room-temperature solid-state lithium batteries. *ACS Appl. Energy Mater.*, 2022, **5**, 2484-2494.

<https://doi.org/10.1021/acsaem.1c04001>